Evaluation of crop transpiration with remote sensing and computer simulation models

J.W. Miltenburg
W. Beekman

Report 1

The WINAND STARING CENTRE, Wageningen, The Netherlands, 1989.

ABSTRACT: Miltenburg, J.W. & W. Beekman, 1989. Evaluation of crop transpiration with remote sensing and computer simulation models. Wageningen, The Netherlands, The WINAND STARING CENTRE. Report 1. 50 p., 10 Fig., 3 Tab., 3 Plates.

A Geo Information System is developed in which remotely sensed imagery is used to extrapolate and verify agro-hydrological model simulations. As hydrological models themselfs are usually well calibrated they need no verification. Input for the models, however, often consists of estimated and generalized standard parameters which need to be verified, especially when simulation results are spatially extrapolated.

A one-dimensional model is applied to simulate crop transpiration for different soil types. Simulation maps are obtained by combining model results with a digital soil map and a land use map. A land use map is obtained through classification of reflection images. Digital reflection and thermal airborne scanner images are used - after radiometric and geometric corrections - to map actual crop transpiration. For a flight day simulated transpiration is verified with the remote sensing derived transpiration map. From this comparison it followed that with model simulations the transpiration for crops on Plaggen soils was overestimated. When model input parameters are adjusted, new, improved, simulations can be performed.

It was found that in general an important improvement of the hydrological description of an area can be achieved by a combination of remote sensing data and hydrological model simulations. Future research should be directed towards the minimisation and assessment of errors due to the combined use of maps and remote sensing data in the developed GIS.

Subject headings: crop transipration, remote sensing, computer simulation.

ISSN 0924-3062

The WINAND STARING CENTRE is continuing the research of: ICW (Institute for Land and Water Management Research), IOB (Institute for Pesticide Research, Environment Division), LB (Division of Landscape Planning, Dorschkamp Research Institute for Forestry and landscape Planning), STIBOKA (Soil Survey Institute).

CONTENTS

Abstract		4
PREFACE		7
1	INTRODUCTION	9
2	TEST SITE, MATERIALS AND EQUIPMENT	11
3	INTEGRATION OF REMOTELY SENSED IMAGERY AND HYDROLOGICAL SIMULATIONS IN A GEO INFORMATION SYSTEM	13
4	IMAGE PROCESSING	15
4.1	Required Remote Sensing Data	15
4.2	Radiometric Correction	17
4.3	Geometric Correction	18
4.4	Classification of Crop Type and Height	21
5	TRANSPIRATION MAPPING WITH REMOTELY SENSED IMAGERY	23
6	TRANSPIRATION SIMULATION	25
6.1	Description of Simulation Model	25
6.2	Model Input	26
6.3	Model Output and Verification	27
7	COMPARISON OF SIMULATED AND REMOTE SENSING DERIVED TRANSPIRATION	29
7.1	Preparation of Transpiration Maps	29
7.2	Results of Comparison	30
8	CONCLUSIONS AND DISCUSSION	37
Plates		39
References		47
Annex		49

PREFACE

The research presented in this paper has been performed in de framework of the Rural Land Use Collaborative Programme of the Joint Research Centre, Ispra, Italy.

1 INTRODUCTION

Information on regional crop transpiration is important for an optimal water management in agriculture. In principle there are two methods to obtain information on actual crop transpiration over larger areas. First, application of agro-hydrological simulation models and second, application of remote sensing techniques.

One-dimensional simulation models have the advantage that they provide information on crop transpiration throughout the growing season, but they do not give any spatial overview. Simulation results can be extrapolated to simulation maps using existing soil maps and land use maps. For flight days, remotely sensed imagery provides information on crop status in terms of patterns. Land use maps are derived from reflective remote sensing data. Transpiration maps can be composed from thermal infrared images, in combination with land use maps. The remote sensing derived transpiration maps can be used to verify model simulations.

Until recently the integration of remote sensing data, existing maps and model simulations was carried out by hand. The main objective of this project is to develop a Geo Information System (GIS) in which hydrological modelling and remotely sensed imagery are combined to make remote sensing techniques operational for larger areas and practical use in water management.

To assess the usefulness of the developed GIS, it is applied in a study presently carried out at the WINAND STARING CENTRE. The aim of this study is to determine the possibilities to save agricultural groundwater consumption in the Province of Noord-Brabant by improved water management, using model simulations. Groundwater can be saved by induced ditch water infiltration during the summer and by using surface water instead of groundwater for sprinkling. Crop water needs are simulated under different boundary conditions so that surface water supply can be estimated. Verification of model simulations is carried out by comparing the map of simulated crop transpiration, one of the components of the water balance, with a transpiration map derived from remotely sensed imagery.

2 TEST SITE, MATERIALS AND EQUIPMENT

The test-area (ca. 100 sq.km) is situated in the south-eastern part of the Netherlands (Province of Noord-Brabant) some 10 km east of the city of Eindhoven. This area was selected because of the availability of data (RS images, digitized soil map). Striking features are formed by a shipping canal, dug in the shallow valley of a small river, crossing the test-area from north-west to south-east and the city of Helmond in the northern part (see Plate 1). Major agricultural crops in the area are grass and maize; potatoes, cereals and sugarbeets occur rarely. The Plaggen and Podzolic soils, developed in the eolian sand deposits covering the area, are drought sensitive. Differences in drainage result from small variations in elevation and texture (fine and loamy fine sand). In the lower central part of the test-area, along the canal, Peat soils are found.

Remote Sensing Products:
- Daedalus Airborne Scanner (DS 1240/1260) band 5, 7, 9 and 12 (resp. green/yellow, red, near infrared and thermal infrared), date: 22-07-1983, flying height: 4000 m, resolution: ca. 10 m, acquisition time: 12.00 MET;
- False Colour Photographs, date: 22-07-1983, flying height: 4000 m, scale: 1 : 26,400.

Maps:
- Soil Map; sheet: 51 east, scale 1 : 50,000 (digitized);
- Topographic Map; sheet: 51 east, scale 1 : 50,000 and 1 : 25,000.

Equipment:
- ERDAS Image Processing System for raster operations on PC and VAX; a Toolkit of subroutines supports the development of software by users of the system;
- ARC/INFO Geo Information System for digitization and vector operations; ARC/INFO and ERDAS are linked together through ETHERNET.

Agro-hydrological Simulation Model:
- The model SWW simulates one-dimensional, non-stationary the water balance in the unsaturated zone (including the interaction with surface water), water uptake by crops and crop production. SWW is derived from the older SWATRE model (FEDDES et al. 1978).

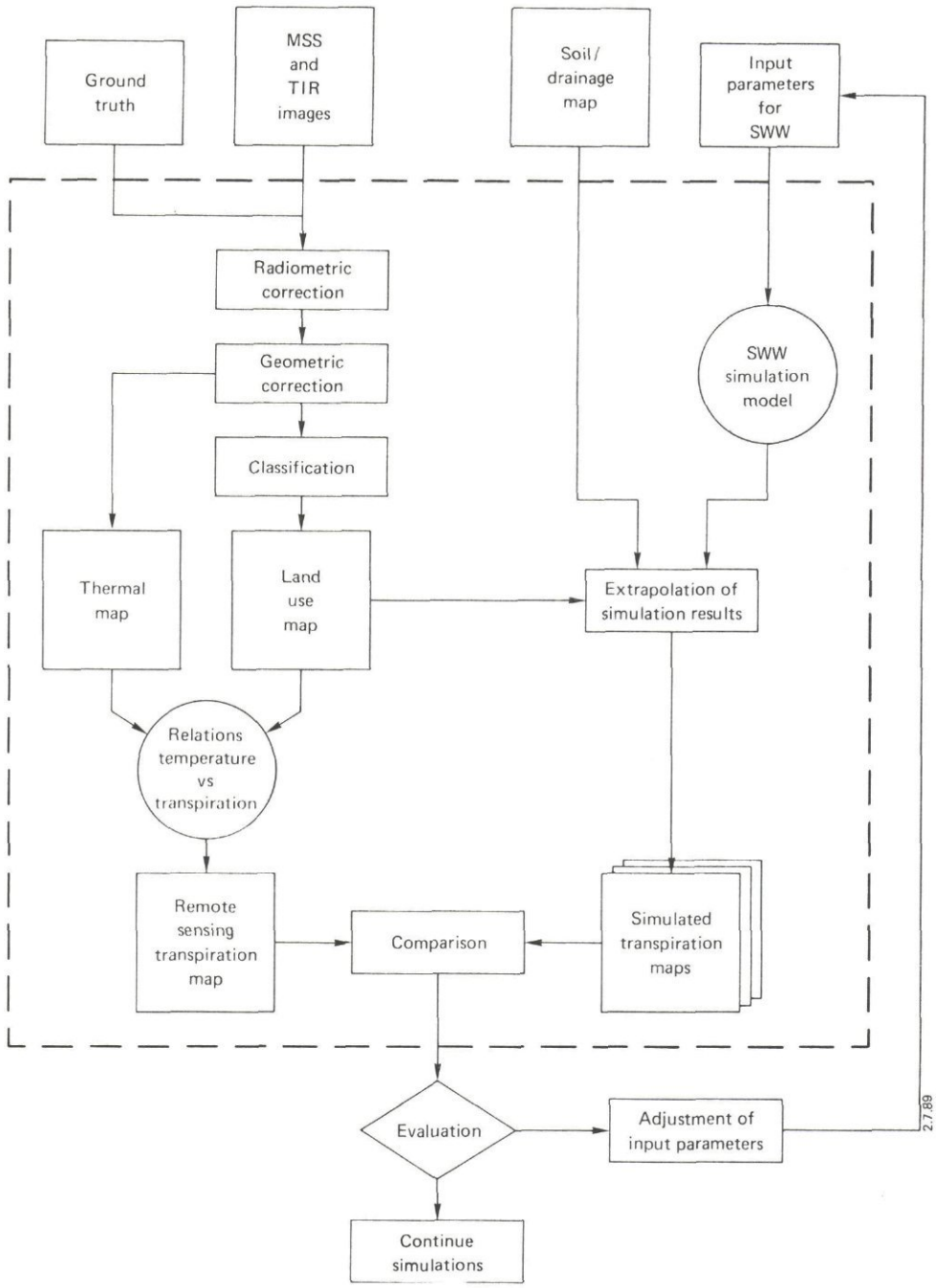

Fig. 1 Flow diagram of the Geo Information System in which model simulations and remotely sensed imagery are combined.

3 INTEGRATION OF REMOTELY SENSED IMAGERY AND HYDROLOGICAL SIMULATIONS IN A GEO INFORMATION SYSTEM

The purpose of this project is to combine model simulations and remote sensing data in a Geo Information System (see Fig. 1). In this system transpiration maps based on remote sensing are used to verify model simulations for a representative test-area on one or two days during a growing season. Input for the GIS consists of: remote sensing images, ground truth, a digital soil/drainage map and simulation model input parameters.

As the SWW-model is well calibrated with accurately measured soil physical, hydrological, meteorological and crop parameters, the model itself needs no verification.

But actually measured input parameters are usually not available over large areas, so readily available standard parameters and generalized soil/drainage maps are used. Because of this input, model results have to be verified. Especially the accuracy of estimated soil physical parameters and rooting depths are important because they strongly influence simulation results.

Model simulations are performed for every so-called simulation-unit. Simulation-units are units in which the water supply to crops is comparable. In practise simulation-units are unique combinations of soil class, crop type and drainage condition. To extrapolate model simulations it is therefore necessary to know the spatial distribution of soil classes, crop types and drainage conditions. The distribution of crop types, which differs from year to year, can be extracted from classified RS imagery. Soil and drainage classes are available on digitized soil maps. More information on simulation model input is given in Ch.6.2.

To perform a transpiration mapping based on remote sensing, according to the method described by NIEUWENHUIS (1986b) and THUNNISSEN AND NIEUWENHUIS (1989), reflective and thermal images are needed. The selection and processing of these images is discussed in Ch.4; the transpiration mapping in Ch.5.

If, after careful evaluation, proof is found for the existence of systematic differences between the simulated transpiration map and the remote sensing transpiration map, model input can be adjusted to improve the simulations. Once model results correspond to the RS transpiration map, simulations can be performed for larger areas.

For this project RS images are available recorded on 22-07-1983. They cover a test-area of ca. 100 sq.km out of the total study-area of 4000 sq.km. Model simulations are performed for every day of the growing season of 1983. Simulation maps are made for 22-07-1983 and also for 26-07-1983, simulating 4 days without precipitation. The latter simulation map is used as an extra aid to assess the sensitivity of the transpiration simulation.

4 IMAGE PROCESSING

4.1 Required Remote Sensing Data

Remote sensing data can be used to (1) extrapolate and (2) verify model calculations.

ad 1.
A land use classification from RS imagery and a digitized soil/drainage map are used to extrapolate the one-dimensional model simulations to simulation maps. The selection of RS data depends on the spatial, spectral and temporal resolution necessary to extract the information needed. As the agricultural fields within the test-area measure between 1 and 10 ha with a maximum of 25 ha, only earth observation satellite systems as SPOT and TM and airborne sensors are potential data sources. The spectral and temporal resolution of the RS images must be such that the two major crops (maize and grass) can be separated without difficulties and that grass height can be determined.

It was found that for the classification of grass and maize TM bands 3, 4 and 5 are a good combination. THUNNISSEN and SCHOUMANS (1988) claim an accuracy of about 90% for maize and grass in large scale agricultural areas, using a supervised maximum likelihood classifier. This result must be close to the maximum possible accuracy, given the effect of always present mixed pixels. An other method is to combine a spring SPOT scene with a summer Daedalus image. This multi-temporal combination can only be applied since a new program for geometrical correction was developed (see Ch.4.3). JANSSEN (1989) found a crop classification accuracy for SPOT/Daedalus of 84% for grass and 78% for maize in a small scale agricultural area. From earlier work (CARIS and JANSSEN 1986) it can be concluded that

Table 1 Spectral bands of the Daedalus scanner (DS 1240/1260) and Landsat-TM.

BandNr	Daedalus	Landsat-TM
1	0.38 - 0.42	0.45 - 0.52
2	0.42 - 0.45	0.52 - 0.60
3	0.45 - 0.50	0.63 - 0.69
4	0.50 - 0.55	0.76 - 0.90
5	0.55 - 0.60	1.55 - 1.75
6	0.60 - 0.65	10.40 -12.50
7	0.65 - 0.69	2.08 - 2.35
8	0.70 - 0.79	
9	0.80 - 0.89	
10	0.92 - 1.10	
11	3.00 - 5.50	
12	8.00 -14.00	

the combination of Daedalus bands 5, 7 and 9 is far from optimal for land use classification (see also Ch.4.4). It seems that the good classification results for grass and maize of TM in comparison to Daedalus must be attributed to TM band 5 (middle infrared). The Daedalus scanner lacks a spectral band in the middle infrared range (see Table 1).

Grass height can be determined using a vegetation index calculated from Daedalus bands 7 and 9 (see Ch.4.4).

ad 2.
NIEUWENHUIS (1986a) found that an actual crop transpiration map can be extracted from Thermal InfraRed (TIR) images, which offers a relatively simple means of verification of simulated transpiration on flight days. Which in turn gives an indication of the correctness of other simulation results in water balance studies (e.g. groundwatertable level). Verification is time and money consuming in the traditional way (fieldwork).

Transpiration mapping with TIR images is based on the fact that crops with sufficient water supply have a higher relative transpiration and therefore a lower temperature than crops in areas with water shortage (see Ch.5).

Concerning the TIR data there is an important constraint namely the time of recording. The optimal aquisition time to detect crop stress conditions due to drought is when the incoming solar radiation flux is maximal, that is at early afternoon, on a clear summer day after a dry period. This means that the thermal band of TM (aquisition time is 10.30 AM) is not suitable. Moreover the spatial and temporal resolution of this band is too poor for respectively the intensively used agricultural land and the humid, cloudy climate which are found in the Netherlands. Even with stand-by aeroplanes it is sometimes impossible to obtain imagery because no dry period followed by a cloud-free day occurs during the entire summer. This and the high costs of airborne imagery are the major limitations that prevent the described method of transpiration mapping from becoming operational on a larger scale.

Given the under 1 and 2 mentioned boundary conditions the optimal RS data set as input for the GIS consists of TM bands 3, 4 and 5 or SPOT bands 1, 2 and 3 in combination with Daedalus bands 5, 7 and 9 for crop mapping. For transpiration mapping in addition Daedalus band 12 (TIR) is necessary. All the images have to be recorded in the same growing season. This combination, however, is at this moment not available for the test-area. It was nevertheless possible to make a transpiration map for 22-07-1983 using only Daedalus images. As already mentioned, crop classification with a Daedalus image only gives rise to problems which will be discussed in Ch.4.4.

The first thing to do was to prepare all ingredients for integration into the GIS. In order to combine RS images with

maps properly, all images have to be registrated to the same coordinate system, in this case the Dutch National Rectangular Coordinate System (stereographic projection).

The quality of the airborne scanner images was such that new software had to be developed for radiometric and geometric corrections. The ERDAS software is developed for satellite images; the radiometric and geometric correction routines are not powerful enough for badly distorted airborne scanner images.

4.2 Radiometric Correction

In the Daedalus image there is a clear gradient in radiation intensity perpendicular to the flight direction for all bands, except band 12 (see Fig. 2).

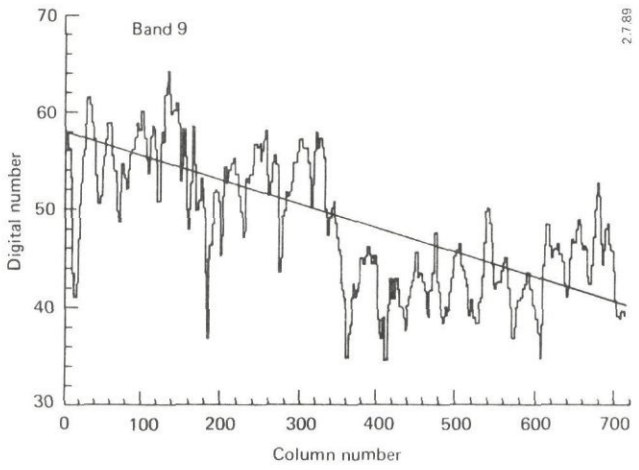

Fig. 2 Gradient of reflection values in the scan direction for Daedalus band 9, and the regression line that is used to estimate the correction values per column.

The reason for this is the large view angle of airborne scanners in combination with a non-optimal flight situation (BARNSLEY 1984). In the optimal flight situation the sun is at its highest point and the flight direction has the same azimuth as the sun (see Fig. 3). During the flight on 22-07-1983 this was not the case and therefore, with the sun somewhat east of the flight-line, the vegetation west of the flight-line reflected more radiation in the direction of the sensor than the vegetation east of the flight-line. This effect depends on wavelength and land use type. The gradient in agricultural fields is conspicuous whereas there is almost no gradient in forested areas.

It is not possible to classify an image showing such a gradient in intensity, so it has to be corrected for. This is achieved

by taking a representative subset of the image, a strip of about 100 lines covering the land use of interest (in this case agricultural fields), calculate the mean pixel values per column and draw a histogram of the mean pixel values vs. column numbers. A linear or second order regression function is fitted and a correction value estimated for every column. In the resulting image the agricultural fields have a quite uniform intensity; for forested areas a gradient is introduced, but this is no serious problem.

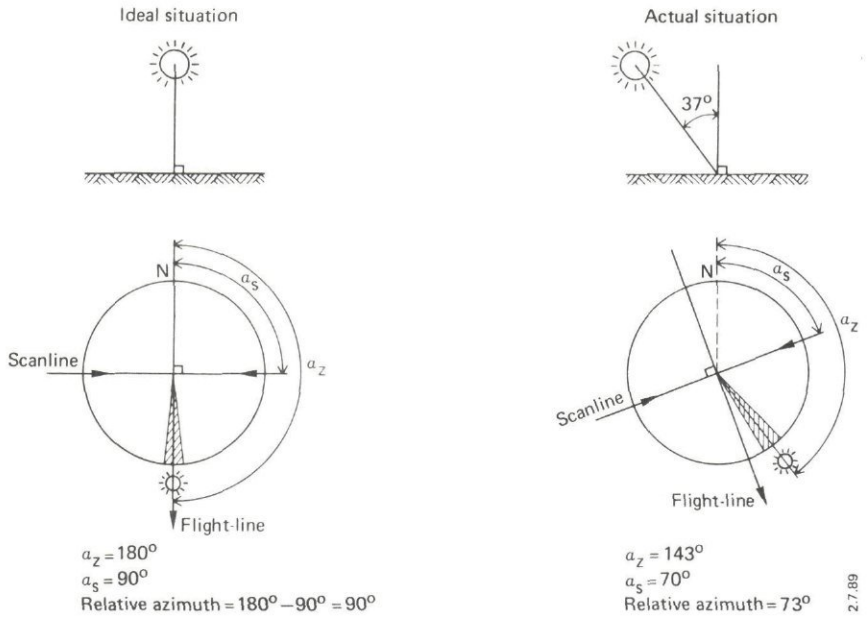

Fig. 3 Position of the sun and direction of the flight-line in an ideal situation and in the actual situation of the scanner flight on 22-07-83, 12.00 MET.

4.3 Geometric Correction

During the scanning process a number of geometric distortions are introduced into airborne scanner data. They can be divided in systematic and non-systematic distortions. The systematic distortions such as panoramic distortion, are known and constant so that they can be corrected for easily.

Non-systematic distortions result from platform movements which are not constant nor known, and can only be corrected using Ground Control Points (GCP's). Low altitude aircraft are very unstable (compared to satellites) and therefore airborne scanner images usually have a very bad geometry, so that geometric correction is a serious problem.

The available ERDAS software (version 7.3) for geometric corrections uses first or higher order polynomial functions. For a first order polynomial 3 GCP's are needed to establish

exactly the coefficients of the transformation function. For a second or third order polynomial the number of GCP's for exact fit are resp. 6 and 10. If more GCP's are used estimates for all coefficients are made using a best fit (usually least squares). Normally a third order function is used as upper limit; polynomials of a higher order tend to oscillate between the GCP's, causing large errors. Using the method of polynomial interpolation the assumption is made that the distortions are of a gentle rolling nature; if there are abrupt changes to be expected, no polynomial function can describe the distortions.

Correction of a relatively small area of about 4 * 6 km from the Daedalus image (with a pixel size of 11 * 6 m), using a third order polynomial resulted in an average displacement of 2.5 pixel over 35 GCP's. From the Topographic Map the main roads and canals were digitized and displayed on top of the rectified image. This showed that displacements of 7-9 pixels occured between the GCP's. However, when trying to correct larger areas, up to 100 sq.km with 200 GCP's the performance of the correction program decreased rapidly, showing maximum displacements of more than 180 m in X and more than 100 m in Y direction with a mean RMS error of 78 m. This result was to be expected because the distortions in the image are local and abrupt; they cannot be corrected using only one function for the whole image. Until now this problem was solved by splitting up the image in smaller sub-images, perform a correction on every sub-image and mosaic these into an output file. This is of course a troublesome method and it can result in displacements on the stitches.

In order to find a definitive solution, if there is one, for the problem of geometric correction of airborne scanner images, the ideas which were formulated in the LIGIS project were picked up. In the LIGIS project some dutch institutes, including the ICW (presently WINAND STARING CENTRE), participated to solve problems occuring when remotely sensed imagery is combined with other data (BROUWER and KENGEN 1988). In co-operation with the Dept. of Surveying and Remote Sensing of the Agricultural University of Wageningen (LUW) these ideas were implemented in the program FATRAS which runs within the ERDAS package on PC-AT.

This new method of geometric correction is not based on one higher order polynomial function but on a large number of first order functions. Between the GCP's triangles (facets) are formed (see Fig. 4), the cornerpoints of every facet form the three co-ordinate pairs needed to fit a first order transformation function for the pixels within the triangle. The performance of this correction method depends for a great deal on the geometry of the triangles. The algorithm used to make triangles out of the GCP's tries to find triangles with equal sides. As can be seen in Fig. 4 this becomes difficult at the

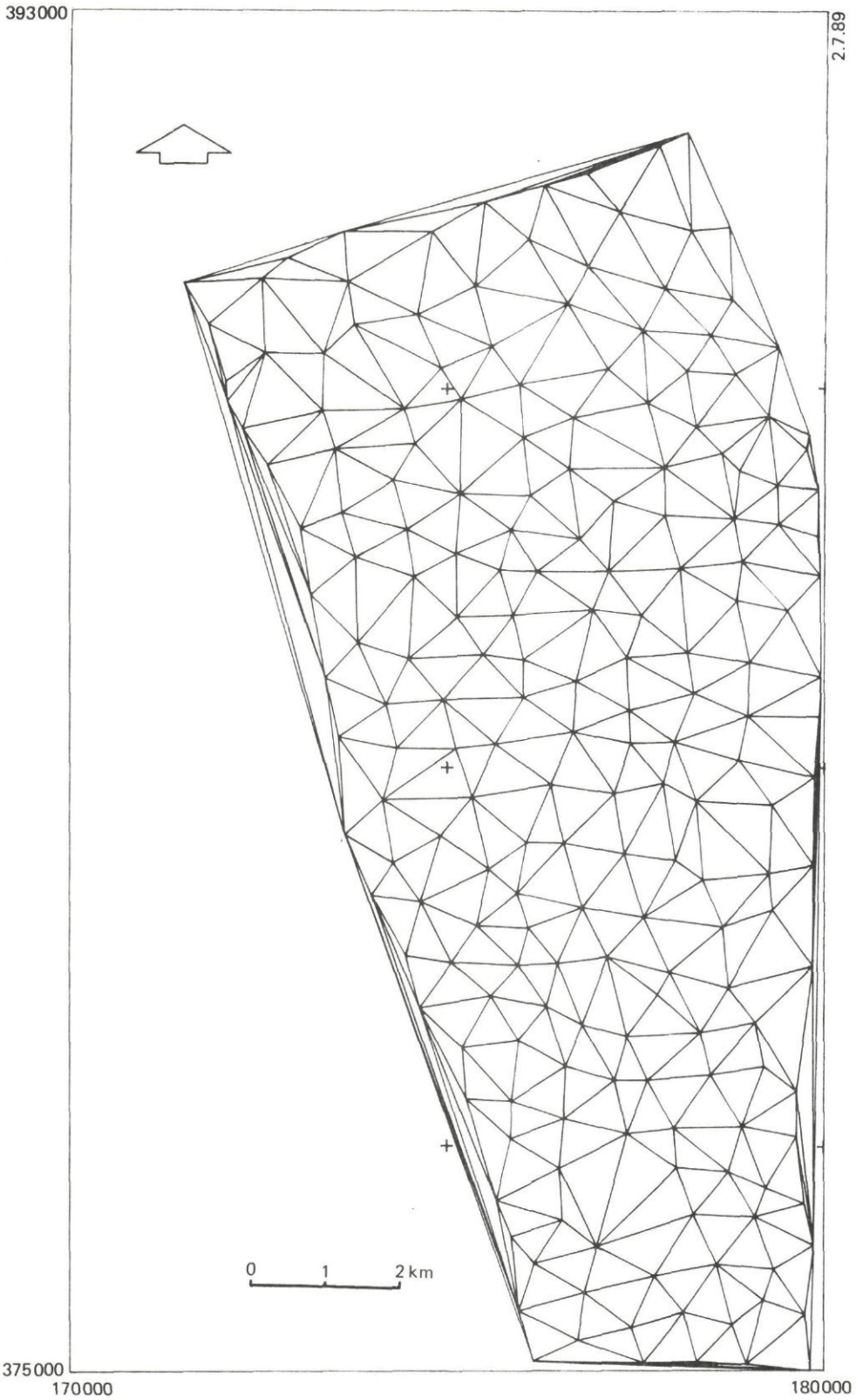

Fig. 4 Plot of the facets formed by the geometrical correction program FATRAS.

sides of the image where often elongated facets are found. The parts of the image covered by these elongated facets show distortions after correction. Therefore only the inner part of the corrected image can be used. This can hardly be seen as a big disadvantage because usually there is enough overlap between neighbouring runs.

Advantages of the facet transformation program FATRAS are:
- local distortions can be corrected by adding new GCP's on troublesome places. Every new GCP adds three new triangles and three new functions, whereas adding extra GCP's to a large number of GCP's when applying a higher order polynomial function, gives almost no improvement;
- the accuracy of correcting a small area is equal to the accuracy of correcting a large area, whereas using higher order polynomials the accuracy decreases as the size of the image increases.

It can be imagined that the transformation of a raster image in this way puts serious demands on computer power (PC-AT) and is therefore time consuming. To make the program more userfriendly it is extended with an option to registrate a digitized map in vector format to a not corrected RS image. This is a relatively fast process (5-10 min.); after displaying the transformed map on top of the image the accuracy of the correction can be assessed visually. If the accuracy is not sufficient new GCP's are added until the required accuracy is reached and the (computer)time consuming image to map registration can be performed.

The final result of the geometric correction of the Daedalus image was reached with 242 GCP's (2.3 GCP per square km) and resulted in a mean RMS error of 24 m (2.4 pixels), with a maximum displacement of 50 m in X and 60 m in Y (these values are determined using 40 random check points). Given the effort of collecting more GCP's and given the average parcel-size and accuracy of other input data for the information system, this result is satisfying for our purpose. Plate 1 shows the radio- and geometrically corrected Daedalus image of the test-area.

The choice between Nearest Neighbour (NN), Bilinear Interpolation and Cubic Convolution resampling techniques was in favour of the first. NN is the only option which does not change the Digital Numbers of the original image; the other two options apply a kind of smoothing which might be more pleasing for the eye, but changes the information content of the image. Another advantage of NN resampling is that it is the fastest resampling technique.

4.4 Classification of Crop Type and Height

The Daedalus MSS-image was classified into 5 classes (maize, grass, forest, bare soil and built-up area), using a maximum

likelihood algorithm. The results were poor as expected. As there is no groundtruth available for 1983 it was not possible to quantify the classification (in)accuracy. The results could only be compared with the False Colour (FC) photographs. For this project only maize and grass parcels needed to be classified; the other classes were of minor importance. Grass was classified relatively good, but a large part of the maize acreage was classified as grass. Therefore the classification result was corrected interactively, based on a visual interpretation of FC photographs. The next step was the application of a filter to remove clumps of maize pixels smaller than a certain threshold.

For the transpiration mapping it is necessary to split 'grass' up into 'short grass' (< 5 cm), 'middle high grass' (5-15 cm) and 'long grass' (> 15 cm). Therefore a Vegetation Index (VI) image is derived from the Red (R) and Near InfraRed (NIR) bands (resp. Daedalus bands 7 and 9), according to:

$$VI = (NIR - R) / (NIR + R) \quad (1)$$

In previous research it was found that a relation exists between VI and crop height (PROJECTTEAM REMOTE SENSING STUDIEPROJECT OOST-GELDERLAND 1985). Based on FC photographs the range of VI-values was subdivided into three classes. Overlaying this subdivision with the classified image resulted in a final land use map with 7 classes (see Table 2 and Plate 1).

Table 2 Land use of Helmond test-area in hectares and percentages of total.

Land use	ha	%
Maize	988.5	12.1
Short grass	979.2	12.0
Middle high grass	1900.2	23.2
Long grass	510.7	6.2
Forest	1601.2	19.5
Built-up and water	1151.5	14.1
Bare soil	1061.9	13.0

As already mentioned it was not possible to quantify the accuracy of the land use map, but with the available materials this was the best possible result. A National Land Cover Mapping Programme with satellite images is carried out now for the Netherlands, so that in the future up to date land use maps can be retrieved from a database. Also the digitization of topographical maps is continuing, this will make it possible to apply an object based post-classification program (JANSSEN et al. in prep.) which improves classification results considerable.

5 TRANSPIRATION MAPPING WITH REMOTELY SENSED IMAGERY

The theory of the method used for the crop transpiration mapping is described by NIEUWENHUIS (1986b) and THUNNISSEN and NIEUWENHUIS (1989). The value mapped is the 24-hour relative transpiration, defined as 24-hour actual transpiration divided by 24-hour potential transpiration (that is transpiration under optimal soil moisture conditions).

Base materials for a transpiration map are a land use map and a geometrically corrected TIR image (see Fig. 1). For every crop type (maize, long grass, middle high grass) a relation is needed between Digital Number (DN) of the TIR image and 24-hour Relative Transpiration (RT). In fact each of these relations consists of two relations: first, the relation DN versus Crop Temperature (Tcr) and second, the relation Tcr versus RT. The first, linear, relation is established through reference measurements of surface temperatures during the flight period.

The relation between Tcr and RT was established in earlier experiments with field measurements and simulation models. For common flight days in the Netherlands the following standard linear relationships, derived from the energy balance for the Earth's surface, can be applied (NIEUWENHUIS 1986b and THUNNISSEN and NIEUWENHUIS 1989):

$$RT = (1 - Br(Tcr-Tcr^*)) * 100\ \% \qquad (2)$$

$$Br = a + b.u \qquad (3)$$

Tcr : actual crop temperature
Tcr* : crop temperature under optimal soil moisture conditions
a,b : constants which depend on crop type and crop height
u : wind speed on 2.0 m above groundsurface

Relative transpiration is depending on the warming up of a cropped surface, relative to the temperature of a cropped surface under optimal soil moisture conditions. Fig. 5 shows a graph of the defined relationships.

Below a RT of about 60% the maize leaves are curling so that soil cover decreases. In that case the measured temperature is influenced by the relatively high temperature of bare soil, which is corrected for by bending the curve. A relative transpiration of 25% is seen as a lower boundary; lower levels of mapped transpiration indicate dying off crops. Simulated or mapped RT levels lower than 25% have to be treated carefully since the relationship between measured temperature and transpiration is not linear anymore. Notice also the fact that higher, rougher crops are warming up less than lower, smoother crops with decreasing transpiration due to their lower resistance to heat exchange with the air.

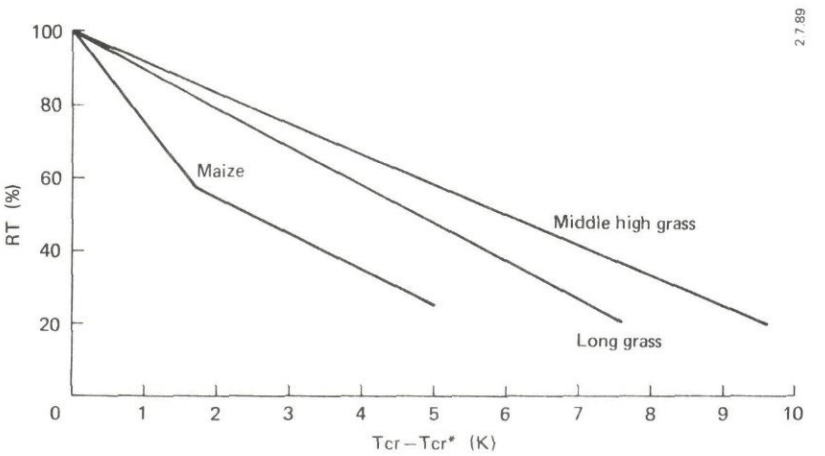

Fig. 5 Relation between relative transpiration (RT) and the increase of crop temperature (Tcr - Tcr) for 22-07-83 in the Helmond test-area.*

As the wind speed is measured during the flight period and the crop parameters are given in literature, Br can be calculated (eq.3). The only unknown parameter remaining, Tcr*, has to be retrieved from the TIR image. This task is liable to subjectivity. First, it is not sure that plots with potentially transpiring crops are found in the scanned area during the flight period and second, there is a high spatial variability in crop temperatures which makes it difficult to find the correct temperature for potentially transpiring crops. Concerning the first point, we are positive that in the lower area along the canal some plots are present with an optimal soil moisture condition. The second point mentioned is solved by taking the average temperature over a parcel instead of the temperature of individual pixels. If all relationships are established, for every crop type look-up tables are made relating its relative transpiration to DN's of the TIR image. Through these look-up tables a transpiration map is created from the TIR image (see Plate 2). For short grass no transpiration values are computed, because short, recently mowed grass has an incomplete soil cover. In that case observed crop temperatures are to a large extent determined by the relatively high temperature of bare soil.

The physical base of this method of transpiration mapping is well established, but in practice there are always deviations from the optimal situation which make it necessary to treat the results with caution. Relative transpiration values should be interpreted as a good indication. Agricultural practices, such as sprinkling irrigation of grassland, result in transpiration values which are much higher than under natural conditions. In that case the effect of soil moisture condition on transpiration is masked and a comparison with simulated transpiration becomes problematic. Sometimes it is possible to identify sprinkled parcels on the FC photographs, so that they can be excluded from the transpiration mapping.

6 TRANSPIRATION SIMULATION

6.1 Description of Simulation Model

SWW is a computer model which was developed as a monitoring instrument for water management by waterboards in the Netherlands. The model consists of two shells. The outer shell prepares the input data for further processing and the output data for presentation. The inner shell consists of the three subsystems of the model:
1 crop transpiration
2 water transport in the unsaturated zone
3 subsurface infiltration.

1 Crop transpiration: Within the crop transpiration subsystem the reference crop transpiration and the potential evaporation are calculated with resp. the Makkink formula or the Penman-Monteith formula. The potential evapotranspiration is derived from this value by multiplying with a crop and time specific factor. The potential transpiration, finally, is derived from the potential evapotrans- piration as a function of the leaf area index (LAI). The LAI is calculated from a crop specific development stage. Crop germination is delayed by too wet or too dry conditions and low temperatures. After germination, too wet or too dry conditions result in a lower transpiration and production rate. During the yield period, water excess hampers mechanized yielding and will cause losses. This is also taken into account in the simulation. More details on this part of the concept can be found in VAN WIJK and FEDDES (1986) and BELMANS et al. (1983).

   The actual crop transpiration is modelled as the sum of the root extractions from the soil compartments within the rooting depth. These extractions are a function of the matrix pressure and the osmotic pressure developed by the crop. The actual soil evaporation is calculated as a function of the water deficit in the top 10 cm of the soil (HOOGLAND et al. 1981 and FEDDES et al. 1978)

2 Water transport in the unsaturated zone: Water transport in the unsaturated zone is modelled only in the vertical direction. The transport of water is simulated by a numerical solution according to the law of Darcy and the continuity equation. The soil profile is subdivided into five soil layers, each of which is subdivided into a number of compartments. The centre points of the compartments are used as the nodes for te numerical solution. For this concept it is necessary to prepare for each layer in the soil profile both the conductivity - pressure head function and the water retention characteristic.

3 Subsurface infiltration: Subsurface infiltration from channels occurs when the channel level is higher than the phreatic level in the bordering landstrip. In the opposite case, drainage

takes place. To fit this proces into an one-dimensional concept, these fluxes are assumed to be vertically directed through the bottom compartment of the unsaturated zone (VAN BAKEL 1986). The rate of infiltration is modelled as a function of the pressure head and the infiltration resistance. The infiltration resistance varies per soil layer and is defined as a function of the channel level, relative to the soil surface. To complete the SWW modelling concepts regional seepage, which can be made time and groundwater level dependent, is added to the infiltration flux.

6.2 Model Input

The SWW-model requires the following input:

1 24-hour meteorological data including precipitation figures and data necessary to calculate potential evapotranspiration.

Meteorological data were all gathered at one station, located centrally within the study-area. The rather high correlation between neighbouring weather stations for radiation, temperature and humidity data makes this generalization to common practice. However daily differences can be rather high, especially precipitation data vary considerably within the total study-area sizing over 4000 sq.km.;

2 crop characteristics such as rooting depth, stomatal resistance and wilting point.

The variety of crops grown in the area was reduced to the two main crops: grass and maize. Without the use of remotely sensed images no topographical location could be assigned to the crops, but per subregion the relative area of both crops is known from agricultural statistics, which enables the estimation of e.g. overall transpiration for a subregion;

3 soil physical parameters including (un)saturated conductivity and water retention characteristics for each soil layer.

The standard 1 : 50,000 soil map of the Netherlands is a generalization of reality; a single unit on this map is usually an association of soil types. Due to map scale and high spatial variability in soil types the chance of actually finding a particular soil type in places where it should be according to the map, is at least 70 %. Soil types are partly classified on colour and chemical properties, therefore a single soil type can include a range of soil physical parameters. Numerous soil samples from all over the country were analysed by the National Soil Survey Institute (presently WINAND STARING CENTRUM) on a routine basis to determine the average soil physical properties per distinguished soil layer (WÖSTEN et al. 1988). The classes displayed on the digital soil map used in this project are based on this analysis and completed with additional measurements. Soil types which showed comparable physical

properties were clustered;

4 groundwatertable regime, which is schematized in a number of drainage classes on the soil map (see Table 3).

The regional seepage level, infiltration resistance and surface-water- system dimensions were found to be correlated to the drainage classes; this information is used in the simulations. Because the drainage classes on the soil map are based on long term means and not on actually measured groundwater levels this may result in inaccuracies in the simulations.

Table 3 Groundwatertable regimes are presented on the standard 1 : 50,000 soil map of the Netherlands in 7 drainage classes based on long term means of measurements of highest groundwater level (MHG) and lowest groundwater level (MLG) per year (in cm below surface).

	1	2	3	4	5	6	7
MHG	<20	<40	<40	>40	<40	40-80	>80
MLG	<50	50-80	80-120	80-120	>120	>120	>160

A number followed by a '*' (e.g. 5*), refers to a dryer part of that particular drainage class.

Resulting soil classes are combined with drainage classes into one map. The unit codes of the soil/drainage map refer to tables with soil parameters and groundwatertable regimes. For the test-area (that is the area covered by the RS images) the soil/drainage map has 54 units. More details on model input are given in the SWW Manual (BEEKMAN et al. 1988).

6.3 Model Output and Verification

On a daily basis the soil water pressure profile is simulated, as well as transpiration rate, groundwater level, drainageflux and surface water level. Weekly transpiration rates are accumulated, as well as other terms of the water balance. For every year, the water balance is totalized and crop production losses are established. Potential crop production is calculated from the weather conditions only, not taking into account soil conditions. Crop production losses due to water stress during germination are calculated from the accumulated daily potential transpiration (including soil conditions) and the optimal potential transpiration (given the weather conditions only). The effects of different water management policies are simulated. From the simulation results the optimal water management is established.

The simulation results can be presented in tables or assigned to a simulation map, which makes the analysis of input data and simulation results suited to be treated within a GIS. In the framework of this project for 22-07-1983 and for 26-07-1983 maps presenting simulated transpiration were composed (see Plate 3).

The SWW-model is calibrated with actually measured input data. For large scale projects only schematized, less accurate input data are available. This makes it necessary to verify model output. The verification of hydrological simulation models is usually performed by comparing the simulation results with actual groundwater levels, as these are easy to measure. THUNNISSEN (1984) and VAN BAKEL (1986), however, state that the verification of actual transpiration is crucial. Assessment of actual transpiration is difficult in the traditional way. Remote sensing provides a useful tool to check transpiration rates and patterns.

7 COMPARISON OF SIMULATED AND REMOTE SENSING DERIVED TRANSPIRATION

A comparison of the two transpiration maps, obtained by respectively model simulation and the remote sensing approach, is necessary to detect the causes of the differences. The differences have to be evaluated carefully to find evidence in favour of one of the two methods. Only if it has been proven that one method gives better results, the other method can be adjusted.

The comparison between the two maps is performed on a pixel by pixel basis, for grass and for maize seperately.
Cross-tabulations are performed giving percentages and numbers of hectares of classes from one map covering a class from another map. Also the mean transpiration values of one map are calculated per class of another map (e.g. soil/drainage map).

7.1 Preparation of Transpiration Maps

The RS transpiration map composed according to the method described in chapter 5 is ready for a visual interpretation of drought patterns. For a pixel by pixel comparison however some pixels have to be removed from the transpiration map. These pixels are non-maize pixels which are mistakenly classified as maize during the manual updating of the classification. They cover parts of roads, bare soil patches within maize parcels and small buildings. These pixels show a much higher temperature than maize pixels and obtain therefore a very low transpiration value, so that the calculation of the mean transpiration over the transpiration map results in a too low value.

Bare soil patches within maize fields can be a result of water excess in spring which hampered germination. With the SWW-model water excess can be simulated but only as a result of high groundwater levels. It is impossible to simulate water excess due to local soil compaction by heavy machinery. The only way to remove all non-maize pixels is to remove all pixels with a relative transpiration lower than 25%. Relative transpiration values less than 25% are hard to interpretate because of dying crops (PROJECTTEAM REMOTE SENSING STUDIEPROJEKT OOST-GELDERLAND 1985) so that it is better to exclude them from the comparison anyway. Calculation of the mean transpiration value over this 'cleaned' map will result in a too high mean transpiration value, because also (parts of) maize parcels with serious water deficits are excluded from the comparison. Therefore, to detect local drought patterns the original transpiration map should be used. In Fig. 6, 7a and 9 two lines are drawn for maize, one indicating the lower and the other indicating the upper boundary of mean RS transpiration; correct

values are found somewhere between the upper and lower boundary.

The maize area used for the comparison was reduced with 20% (to 750 ha.) after exclusion of pixels with a relative transpiration less than 25%. The effect was an increase of the mean relative RS transpiration over the total maize area from 62% to 73% (see Fig. 6) and the mean simulated transpiration from 86% to 92%.

For the classification of grass a Vegetation Index was used and for short grass no transpiration mapping was performed. Therefore no bare soil patches are included in grass parcels and no correction had to be carried out for grass.

7.2 Results of Comparison

Without reference field measurements of actual transpiration it is hard to determine the exact accuracy of the two approaches to map relative transpiration, but the FC photographs do give some information on crop condition. Maize parcels on fertile soils under optimal soil moisture conditions have an even, bright red colour, while maize plots under less favourable conditions have a stained, less bright appearance. A visual comparison of the RS transpiration map with the FC photographs made clear that, at least the relative level of the mapped transpiration corresponds with the patterns on the photographs. For the simulation map the agreement with patterns on the FC photographs was not good. After 3 weeks with high potential evapotranspiration and no rain a considerable reduction in crop transpiration might be expected, but the simulation map indicated potential transpiration for large areas (see Plate 3). Because of these two reasons it is assumed that the transpiration map based on RS is closer to reality.

A visual interpretation of the two transpiration maps of 22-07-83 (Plates 2 and 3) shows that along the indicated shipping canal and in the southern part of the test-area crop water supply is sufficient. Especially around forested areas soils are sensitive to drought. This is not surprising as forested areas were not brought under cultivation because of there sensitivity to drought. The RS transpiration map provides relatively detailed information, while simulations on the basis of a generalized soil map give rougher information. The RS transpiration map is more or less speckled. This is a result of (leveled) within-field relief or other small-scale variations, which can not be simulated. It must be remembered that grass occupies ca. 30% of the test-area and maize only 12% (Table 2). Due to the effect of sprinkling on the RS transpiration for grass, the differences between the two transpiration maps of 22-07-83 on plates 2 and 3 are more or less masked. The great reduction in transpiration that seems to have occurred between 22-07 and 26-07 on the simulation maps (Plate 3) is also mainly

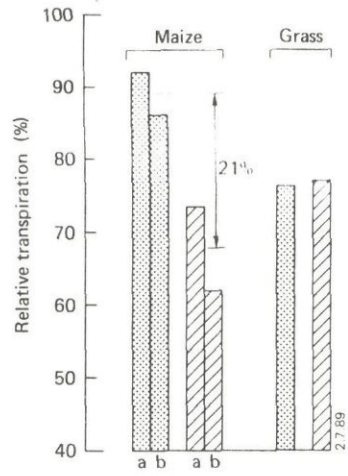

Fig. 6 Mean relative transpiration over the test-area for maize and grass (22-07-83).
▨ simulated transpiration
▨ remote sensing transpiration
a excluded pixels with a transpiration < 25%
b original transpiration map

a result of the large reduction for grass with its shallow rooting depth (see Fig. 10).

Fig. 6 shows that the mean simulated transpiration is more or less equal to the mean RS transpiration for grass, while simulated transpiration for maize is about 21% higher than RS transpiration. Maize parcels are not sprinkled, so that it can be concluded that the simulation model overestimates maize transpiration. From field observations it is known that grass parcels are usually sprinkled during a dry period. Irrigation is not simulated and raises the transpiration of grass on the RS transpiration map; without irrigation, RS transpiration for grass would be lower so that also for grass the transpiration is overestimated by the simulation model.

To illustrate the effect of sprinkling Fig. 7 shows the mean transpiration per drainage class of resp. maize and grass. For maize simulated transpiration is higher for every drainage class, whereas for grass there is some differentiation. Classes 2 and 3 (shallow groundwater = less sprinkling) show an overestimation by the simulation model; classes 7 and 7* (deep groundwater = more sprinkling) show an underestimation by the simulation model. The low transpiration values for drainage class 5* in Fig. 7a and 7b seem to be a result of the fact that most of the area with drainage class 5* coincides with an unfertile soil in relatively coarse sand. High transpiration of maize for drainage class 7 and 7* is a result of fertile soils with a high capillary rise.

Fig. 8 gives a first impression of the differences between simulated and RS transpiration per soil/drainage class. Points were expected to be situated around the indicated line. This is clearly not the case and therefore a more detailed

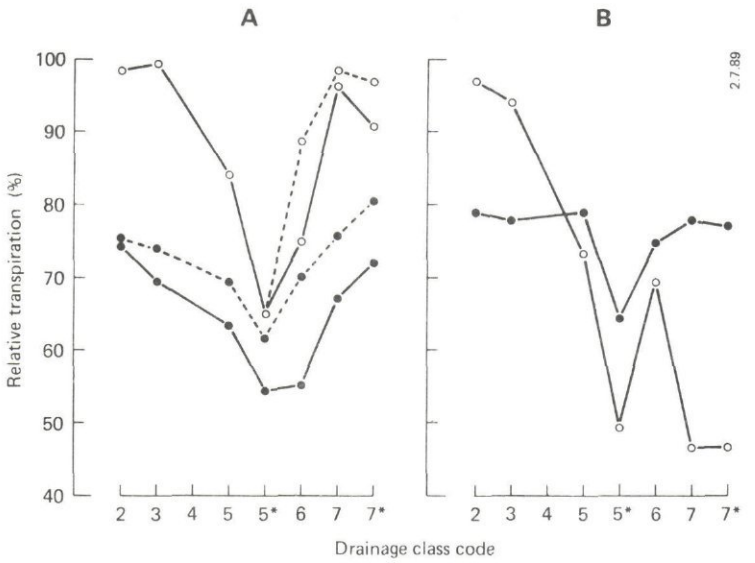

Fig. 7 Mean relative transpiration of maize (A) and grass (B) on 22-07-83, per drainage class (drainage class codes are listed in Table 3).

- •—• remote sensing transpiration
- •---• remote sensing transpiration, excluded pixels with a transpiration < 25%
- o—o simulated transpiration
- o---o simulated transpiration, excluded pixels with a transpiration < 25%

investigation was started. The overestimation of the simulation model is a result of incorrect crop parameters, incorrect soil parameters or both. It is difficult to separate these two groups of parameters because rooting depth depends on soil type. In the case of water excess in spring (which occurred in 1983) it is even possible that rooting depth depends on the drainage class. Because for both, maize and grass, a (hidden) overestimation was found, the overestimation of simulated crop transpiration is assumed not to depend on crop parameters.

To find out if the differences between simulated and RS transpiration have any relation with soil/drainage classes, mean transpiration values per soil/drainage class are plotted in Fig. 9 for maize and Fig. 10 for grass. The soil/drainage classes are ordered from low to high RS transpiration. Simulated transpiration values, especially for gras, have a somewhat wider range than RS transpiration values. Grassland plots are kept moist by the farmers, so that the transpiration rates are constant on a relatively high level (ca.75%). As most of the grassland is irrigated the comparison between the simulation map and RS transpiration map on the basis of soil/drainage classes is mainly restricted to maize.

After a dry period a sharp drop in available soil moisture and therefore crop transpiration can occur suddenly in some soils.

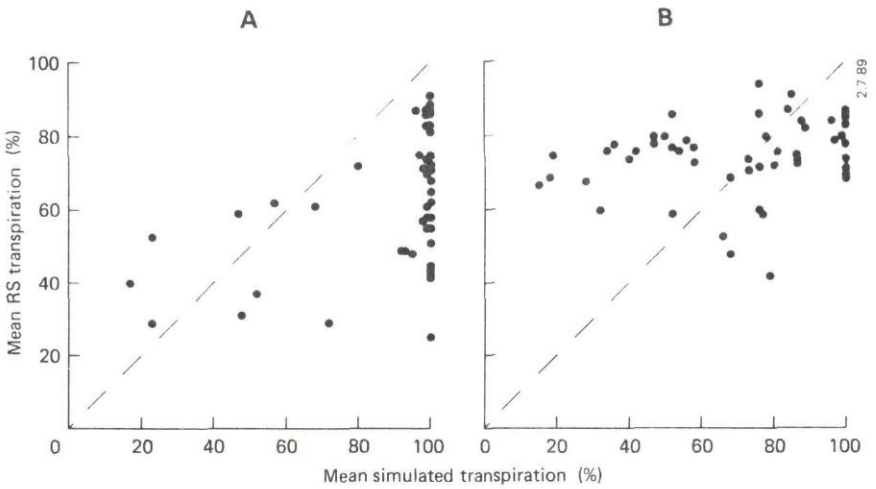

Fig. 8 Mean relative transpiration of maize (A) and grass (B) as obtained by the RS approach versus mean simulated transpiration, for resp. 45 and 52 soil/drainage classes.

Determination of soil physical parameters is therefore critical. In the simulation of the water balance for a whole year daily transpiration (and other) values are accumulated. Given the total amount of transpiration over a year no large errors will arise if a certain level of transpiration is reached one or two days later. Knowing this a simulation map for 26-07-83 was composed, simulating 4 more days without precipitation (see Plate 3), and included in the comparison. Mean values from this map are also shown in Fig. 9 and 10.

For 22-07, 23 out of 45 soil classes show a simulated relative transpiration of 100% for maize while the RS approach shows a (great) reduction in transpiration. For 10 classes simulated transpiration is higher and for 2 classes lower than RS transpiration. For 10 soil/drainage classes both approaches show about the same values (+/- 20%). For 10 soil/drainage classes the simulated transpiration is 100% on both 22-07 and 26-07 and 8 classes show a very small reduction on 26-07, while the RS approach shows already on the first date a clear reduction in transpiration of more than 20%. Other soil classes do show a considerable reduction in simulated transpiration on the second date; as explained above, this can be a result of the critical timing of sudden drops in transpiration.

Due to the effect of irrigation it is more difficult to make the same analysis for grass (see Fig. 10). Soil/drainage classes for which transpiration is overestimated by the SWW-model have, nearly all, a drainage class of 2 or 3; underestimated soil/drainage classes all have a drainage class of 5, 5*, 6, 7 or 7*. For 8 soil/drainage classes out of 52 no reduction in transpiration is found for both dates, while the RS transpiration map, even with irrigation, shows a reduction of 15 to 30%. These 8 soil/drainage classes belong to the same group of classes as was found to overestimate maize transpiration.

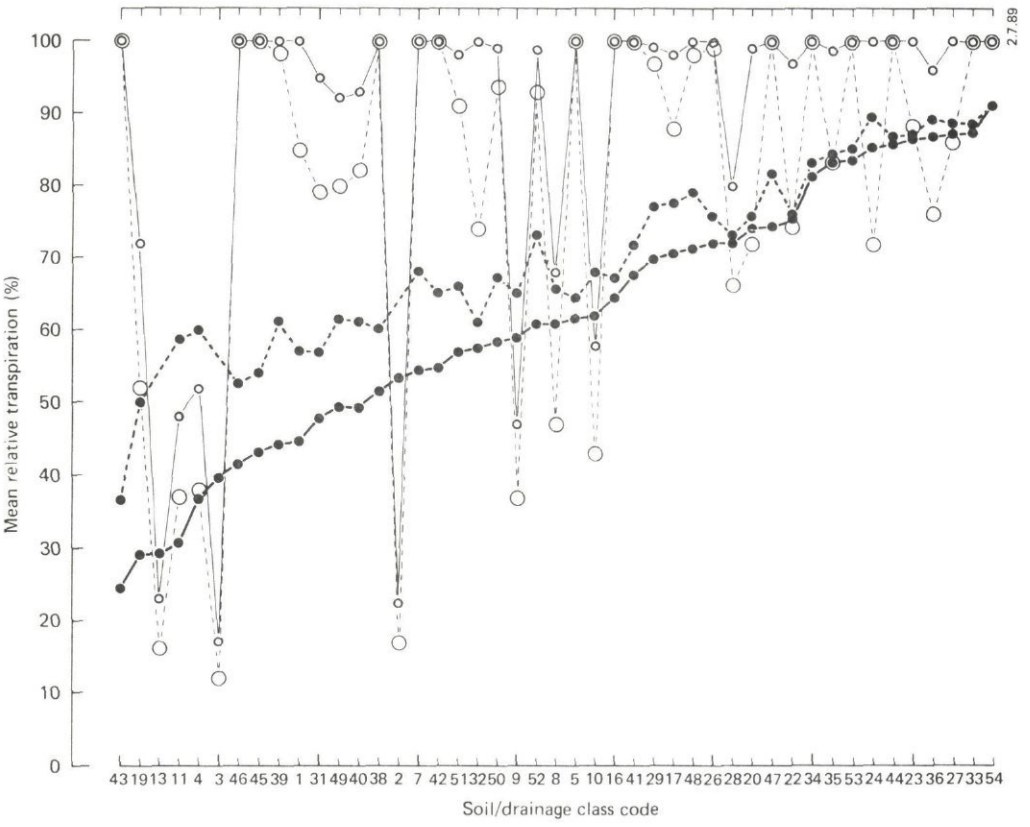

Fig. 9 Mean relative transpiration of maize per soil/drainage class (see Annex for meaning of soil/drainage class codes).

•—• : remote sensing transpiration
•--• : remote sensing transpiration, excluded pixels with a transpiration < 25%
o—o : simulated transpiration (22-07-83)
o--o : simulated transpiration (26-07-83)

The differences per soil/drainage class were related to the original soil types on the soil map. It is not possible to discuss the results for all the different soil/drainage classes in this report (a list of codes is given in the Annex); only some general remarks can be made about this analysis. During the simulation the transpiration for Plaggen soils was overestimated, in numerous cases there was no reduction in transpiration simulated for both dates, while according to the RS approach reduction in transpiration occurred. For Podzolic soils, in contrast, the results of both methods were in good agreement. For Peat soils both methods agreed reasonably, but the number of hectares involved was to small to make a clear judgement.

In previous studies it was also found that crop transpiration was overestimated with simulation models for Plaggen soils REMOTE SENSING STUDIEPROJEKT OOST-GELDERLAND 1985), probably due to a too optimistic estimate of capillary rise and/or rooting depth. It is however not possible to adjust the soil physical parameters of all soil classes involved in a short time. More research is

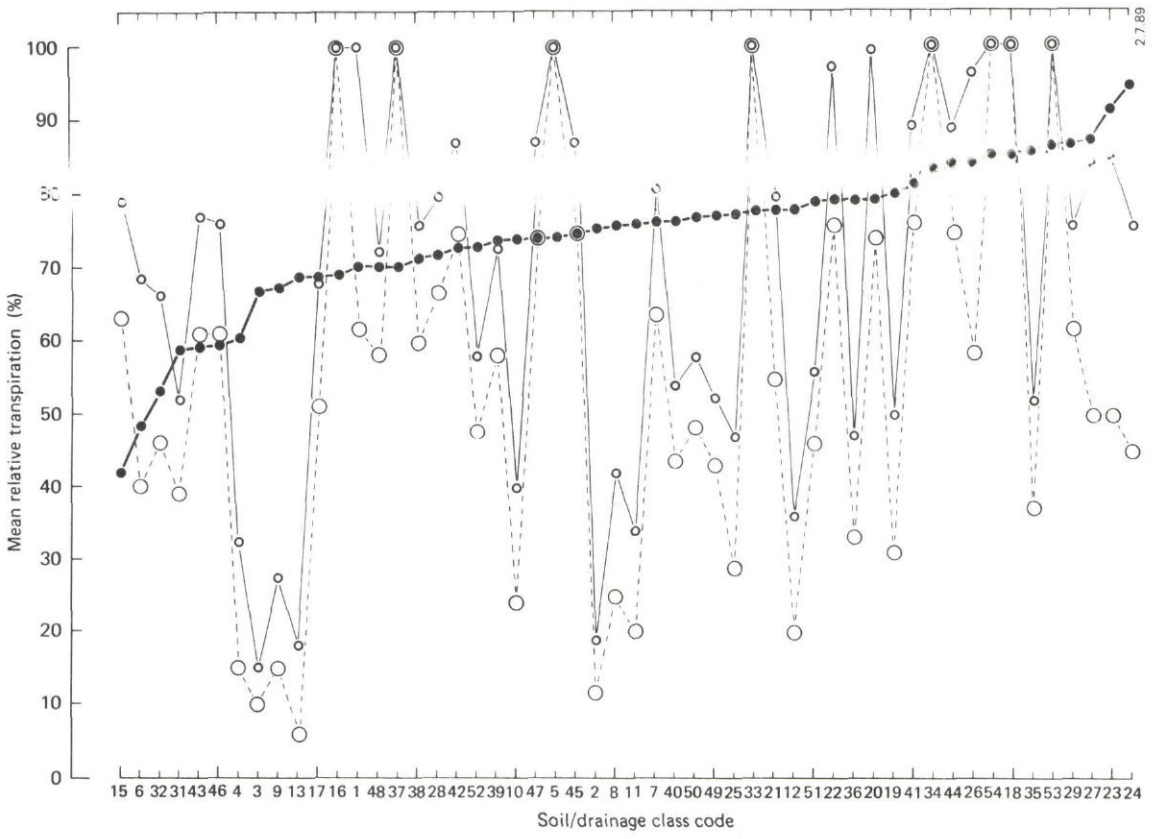

Fig. 10 Mean relative transpiration of grass per soil/drainage class.

necessary to gather improved input parameters and perform new simulations.

8 CONCLUSIONS AND DISCUSSION

The Geo Information System described in this report proved to be a valuable tool for extrapolation and verification of model simulations using remotely sensed data. Second generation earth observation satellites (SGEOS) provide relatively cheap and useful data for crop classification. Thermal imagery for crop transpiration mapping can only be obtained with airborne scanners. Succesful application of the GIS depends on the availability of these remote sensing products. The Dutch climate and the high costs of airborne imagery are major constraints. Radiometric and geometric correction problems are sufficiently solved with the development of new software. Recent developments in the integration of geo information and remote sensing systems and the progress in the digitization of topographical and soil maps in the Netherlands, will make it possible in the near future to apply the developed GIS on a larger scale.

On several places in this report side-notes are made on the accuracy of maps, parameters etc. The propagation of errors is a major problem in GIS applications, and is hard to tackle. This was a first study to find out if a GIS as described was feasible. The available data set was not optimal and no extra ground truth could be obtained as the data set dated from 1983. But already with this data set it was clear that the transpiration of crops on Plaggen soils was overestimated by the simulation model. The overestimation was so evident that it could not be attributed to inaccuracies in the process of image processing, transpiration mapping, extrapolation of simulation results and the comparison of both transpiration maps. More detailed conclusions, however, could not be drawn from this evaluation.

There is already some research available on the accuracy of model simulations and on the method of transpiration mapping based on remote sensing. Therefore should future research be directed towards the minimisation and assessment of errors in the GIS due to the combined use of maps and geometrically corrected images, both with their own accuracy. Also the effect of misclassifications and mixed pixels on the comparison of the RS transpiration map with simulated transpiration should be evaluated. Only if all errors are known and minimised, detailed conclusions on the correctness of model input can be drawn on a solid base.

PLATES

Plate 1 (Left) Radio- and geometrically corrected Daedalus MSS image of 22-07-83 (Combination of bands 5, 7 and 9).

(Right) Land use map of test-area obtained by spectral classification in combination with a Vegetation Index.

Plate 2 (Left) Thermal infrared image (Daedalus band 12) of 22-07-83. Light tones indicate higher temperatures.

(Right) Transpiration map derived from remotely sensed imagery for 22-07-83.

Plate 3 (Left) Simulated transpiration map for 22-07-83.

(Right) Simulated transpiration map for 26-07-83.

[A

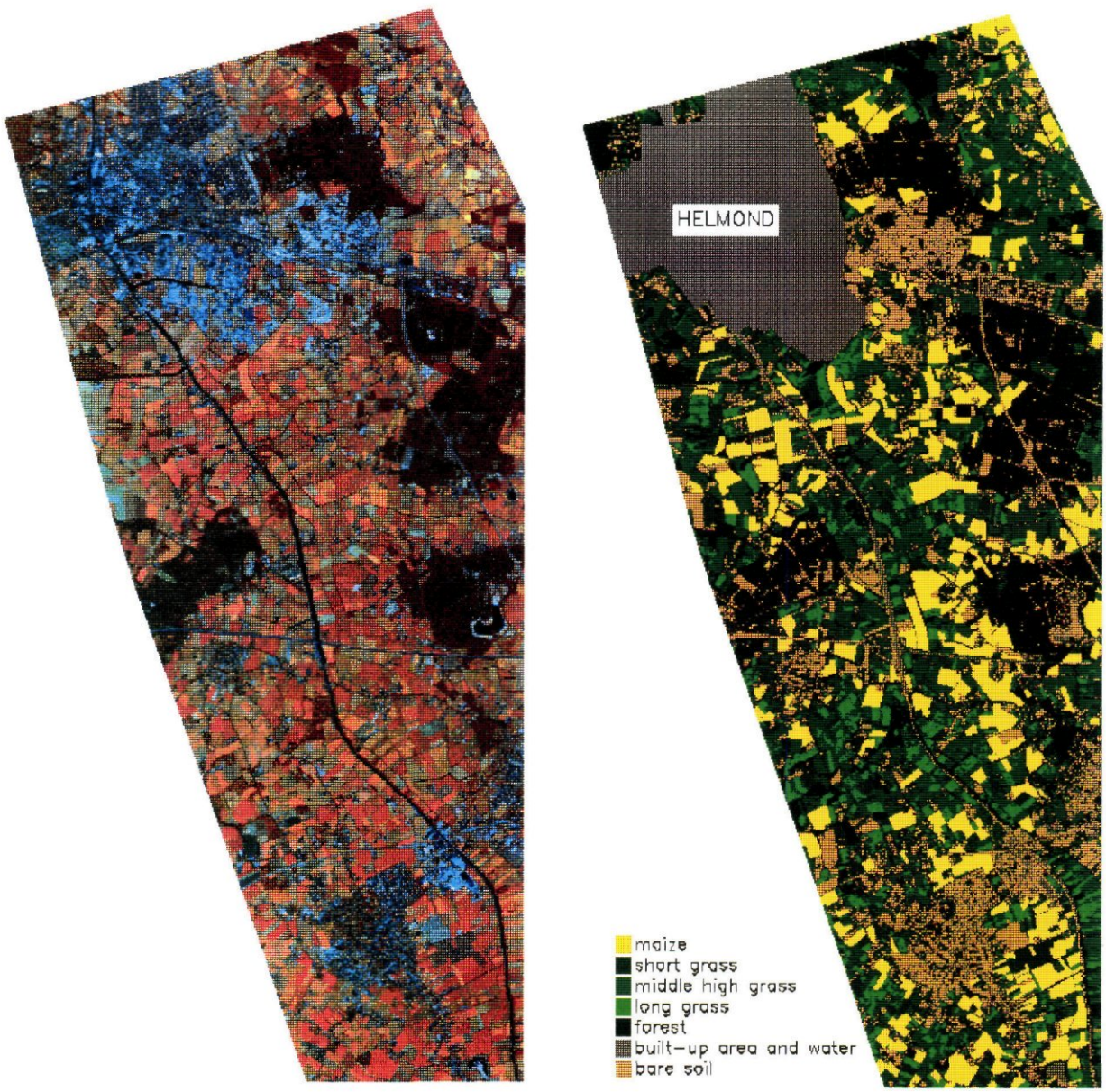
HELMOND
maize
short grass
middle high grass
long grass
forest
built-up area and water
bare soil

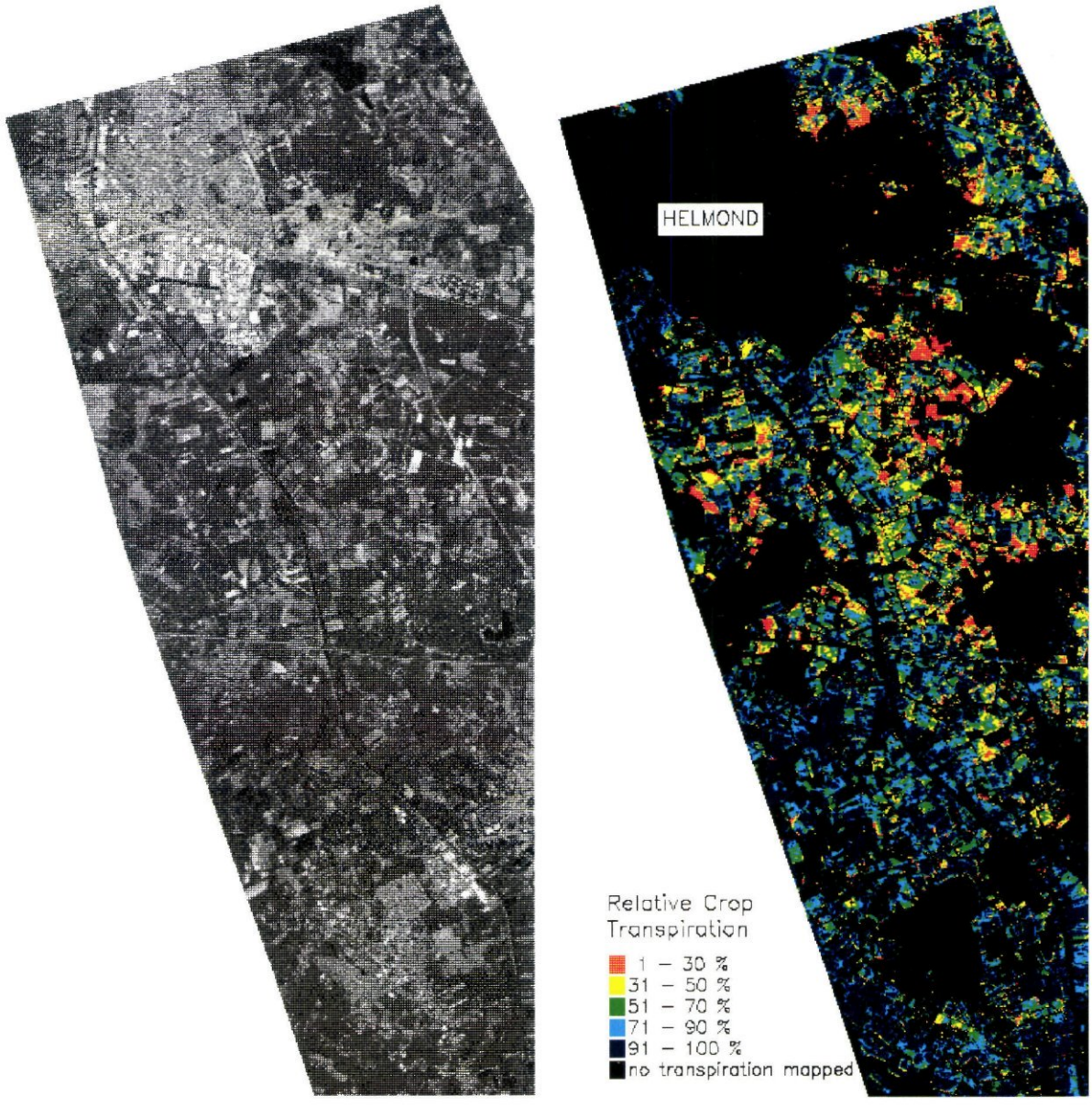
HELMOND
Relative Crop
Transpiration
1 – 30 %
31 – 50 %
51 – 70 %
71 – 90 %
91 – 100 %
no transpiration mapped

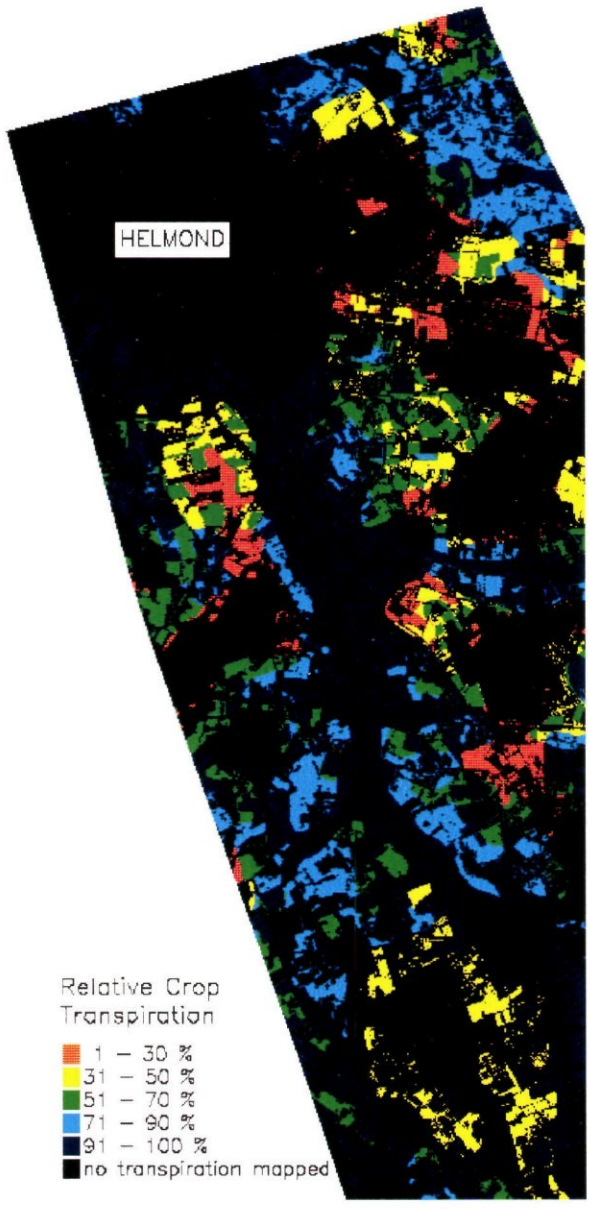
HELMOND
Relative Crop Transpiration
1 – 30 %
31 – 50 %
51 – 70 %
71 – 90 %
91 – 100 %
no transpiration mapped

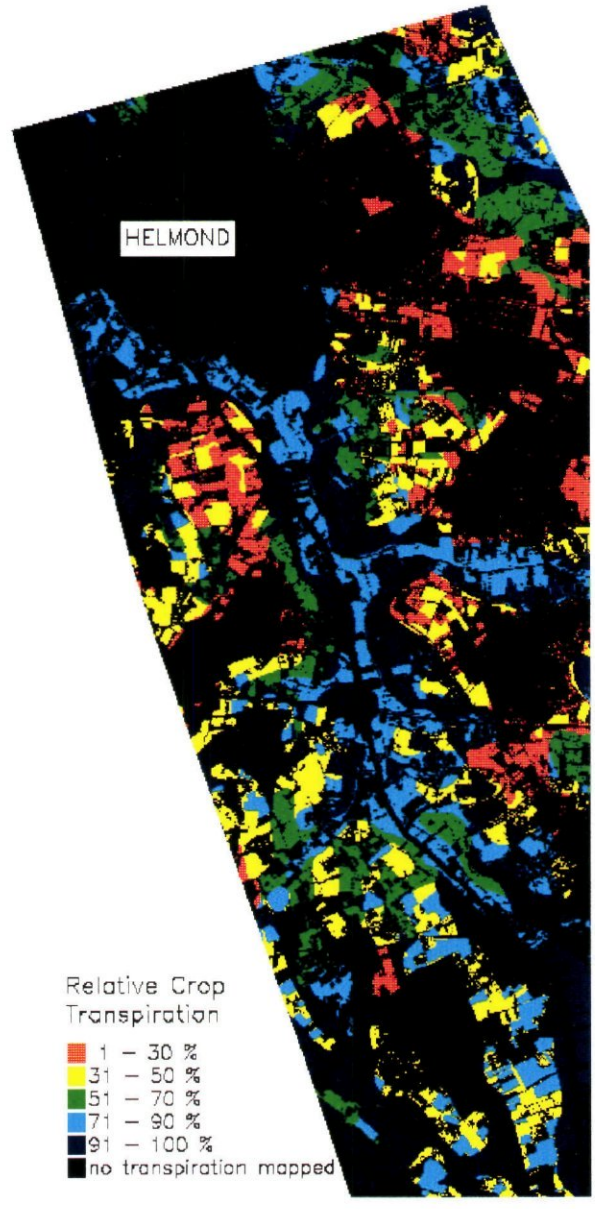
HELMOND
Relative Crop Transpiration
1 – 30 %
31 – 50 %
51 – 70 %
71 – 90 %
91 – 100 %
no transpiration mapped

REFERENCES

BAKEL, P.J.T. VAN, 1986. A systematic approach to improve the planning, design and operation of regional surface water management systems: a case study. ICW Report 13, Wageningen, the Netherlands.

BARNSLEY, M.J., 1984. Integration of multispectral data obtained at different view angles for vegetation analyses. Earsel/Esa Symposium on integrative approaches in remote sensing. ESA sp-214, pp. 135-142.

BEEKMAN W., P.J.T. VAN BAKEL and P. NIJHOF, 1988. Ontwikkeling en toepassing van het simulatiemodel SWW als begeleidingssysteem voor het kwantitatieve oppervlaktewaterbeheer. ICW Nota 1912 (in Dutch).

BELMANS C., J.G. WESSELING and R.A. FEDDES, 1983. Simulation model of the waterbalance of a cropped soil : SWATRE. Journ.Hydr. 63 (3/4): pp.271-286.
Also publ. as: ICW Techn. Bull. 21, Wageningen, the Netherlands.

BROUWER, H. DE and KENGEN, H. 1988. Final report LIGIS research project. ITC, ICW & LUW, Enschede, the Netherlands.

CARIS, J.P.T. and JANSSEN, L.L.F. 1986. Remote sensing verdampingskartering rond peelrandbreuk. ICW nota 1720, Wageningen, the Netherlands.

FEDDES, R.A., KOWALIK, P.J. and ZARADNY, H. 1978. Simulation of field water use and crop yield. 189 p., PUDOC, Wageningen, the Netherlands.

HOOGLAND J., C. BELMANS and R.A. FEDDES, 1981. Root water uptake model depending on soil water pressure head and maximum extraction rate. Acta Hortic. 119: pp.123-126.

JANSSEN L.L.F. 1989. Personal communication.

JANSSEN L.L.F., M.N. JAARSMA, H.T.M. VAN DER LINDEN and P.J. AARNINK. Land cover classification accuracy using geographical information and different scanner types (in prep.).

NIEUWENHUIS, G.J.A. 1986a. Thermography: principles and application in the Oost-Gelderland Remote Sensing Study Project. ITC J.,Vol 1:51-58. Also publ. as: ICW Techn. Bull. 43, Wageningen, the Netherlands.

NIEUWENHUIS, G.J.A. 1986b. Integration of remote sensing with a soil water balance simulation model (SWATRE). IAHS Publ.160. Also publ. as: ICW Techn. Bull. 59, Wageningen, the Netherlands.

PROJECTTEAM REMOTE SENSING STUDIEPROJEKT OOST-GELDERLAND, 1985. Operational applications of remote sensing in agriculture and nature conservation. ICW Report 17 (in dutch). 26 p., Wageningen, the Netherlands.

THUNNISSEN, H.A.M. 1984. Toepassing van hydrologische modellen en remote sensing. Deelrapport 4. ICW Nota 1542, Wageningen, the Netherlands.

THUNNISSEN H.A.M. and G.J.A. NIEUWENHUIS, 1989. An application of remote sensing and soil water balance simulation models to determine the effect of groundwater extraction and crop evapotranspiration. 18 p. Accepted by Agric. Water Management.

THUNNISSEN, H.A.M. and SCHOUMANS, O.F. 1988. Land cover inventory for soil and groundwater protection purposes using remote sensing. ISS Symposium 1988, Budapest, Hungaria.

WIJK A.L.M. VAN and R.A. FEDDES, 1986. Simulating effects of soil type and drainage on arable crop yield. ICW Techn. Bull. 40, Wageningen, the Netherlands.

WÖSTEN J.H.M., M.H. BANNINK and J. BEUVING, 1988. Waterretentie- en doorlatendheidskarakteristieken van boven- en ondergronden in Nederland: De Staringreeks. ICW Rapport 18, Wageningen, the Netherlands.

ANNEX

List of used soil/drainage class codes and their relation with soil type codes in the legend of the Soil Map (1 : 50,000) of the Netherlands and drainage class codes (see Table 3). When the same soil type is listed more than one time, this means that the soil type is subdivided because of different soil physical properties.

Soil/drainage class	Soil type	Drainage class
1	Hn21	3
2	Hn21	6
3	Hn21	7*
4	Hn21	6
5	pZg21	3
6	pZg21	5*
7	kpZg21	3
8	Hn21	5
9	Hn21	5*
10	Hn21	5
11	Hn21	6
12	Hn21	6
13	Hn21	7
14	Hn21	7*
15	Vc	2
16	pZg23	3
17	pZg23	5
18	Hn23	3
19	Hn23	5
20	zVz	2
21	zVz	3
22	zWp	2
23	cHn23	5
24	cHn23	6
25	cHn23	5*
26	Hn23	5
27	Hn23	6
28	vWz	2
29	vWz	3
30	cHn21g	6
31	cHn21	5*
32	cHn23t	6
33	bEZ23	5
34	bEZ23	6
35	bEZ23	7
36	bEZ23	7*
37	zEZ23	6
38	zEZ21	5
39	zEZ21	6
40	zEZ21	7

41	zEZ21	5
42	zEZ21	6
43	zEZ21	5*
44	zEZ21	5
45	zEZ21	6
46	zEZ21	5*
47	zEZ21	6
48	zEZ21	6
49	zEZ21	7*
50	zEZ21	7
51	zEZ21	7*
52	zEZ21	7
53	EZg23w	3
54	EZg23g	3

V and W : Peat soils
H : Podzolic soils
E(Z) : Plaggen soils